



## Journal of Coordination Chemistry

Publication details, including instructions for authors and subscription information:

<http://www.tandfonline.com/loi/gcoo20>

### Water-soluble scorpionate ligands and their reactions with molybdenum complexes. Crystal structures of lithium tris(3-isopropylpyrazol-1-yl)methanesulfonate and $\text{Mo}^{\text{V}}\text{OCl}_3(\text{OPPh}_3)_2 \cdot \text{Mo}^{\text{VI}}\text{O}_2\text{Cl}_2(\text{OPPh}_3)_2$

Lyndal M.R. Jensen<sup>a</sup>, Brendan F. Abrahams<sup>a</sup> & Charles G. Young<sup>a</sup>

<sup>a</sup> School of Chemistry, University of Melbourne, Parkville, Australia

Accepted author version posted online: 25 Feb 2013. Published online: 05 Apr 2013.

To cite this article: Lyndal M.R. Jensen, Brendan F. Abrahams & Charles G. Young (2013) Water-soluble scorpionate ligands and their reactions with molybdenum complexes. Crystal structures of lithium tris(3-isopropylpyrazol-1-yl)methanesulfonate and  $\text{Mo}^{\text{V}}\text{OCl}_3(\text{OPPh}_3)_2 \cdot \text{Mo}^{\text{VI}}\text{O}_2\text{Cl}_2(\text{OPPh}_3)_2$ , Journal of Coordination Chemistry, 66:7, 1252-1263, DOI: [10.1080/00958972.2013.778988](https://doi.org/10.1080/00958972.2013.778988)

To link to this article: <http://dx.doi.org/10.1080/00958972.2013.778988>

PLEASE SCROLL DOWN FOR ARTICLE

Taylor & Francis makes every effort to ensure the accuracy of all the information (the "Content") contained in the publications on our platform. However, Taylor & Francis, our agents, and our licensors make no representations or warranties whatsoever as to the accuracy, completeness, or suitability for any purpose of the Content. Any opinions and views expressed in this publication are the opinions and views of the authors, and are not the views of or endorsed by Taylor & Francis. The accuracy of the Content should not be relied upon and should be independently verified with primary sources of information. Taylor and Francis shall not be liable for any losses, actions, claims, proceedings, demands, costs, expenses, damages, and other liabilities whatsoever or howsoever caused arising directly or indirectly in connection with, in relation to or arising out of the use of the Content.

This article may be used for research, teaching, and private study purposes. Any substantial or systematic reproduction, redistribution, reselling, loan, sub-licensing,



# Water-soluble scorpionate ligands and their reactions with molybdenum complexes. Crystal structures of lithium tris(3-isopropylpyrazol-1-yl)methanesulfonate and $\text{Mo}^{\text{V}}\text{OCl}_3(\text{OPPh}_3)_2 \cdot \text{Mo}^{\text{VI}}\text{O}_2\text{Cl}_2(\text{OPPh}_3)_2$

LYNDAL M.R. JENSEN, BRENDAN F. ABRAHAMS and CHARLES G. YOUNG\*

School of Chemistry, University of Melbourne, Parkville, Australia

(Received 16 December 2012; in final form 1 February 2013)

The water soluble ligands, lithium and potassium tris(3-isopropylpyrazol-1-yl)methanesulfonate ( $\text{LiTpms}^{\text{iPr}}$  and  $\text{KTpms}^{\text{iPr}}$ ) and potassium hydrotris(3-carboxyethyl-5-methylpyrazol-1-yl)borate ( $\text{KTP}^{\text{CO}_2\text{Et,Me}}$ ), have been prepared and their reactions with simple Mo-containing starting material investigated. The crystal structure of  $\text{LiTpms}^{\text{iPr}} \cdot 1.2\text{MeOH}$  consists of dinuclear units containing two distinctly different, four-coordinate, tetrahedral Li centers coordinated by bidentate  $\kappa^2\text{N,O-Tpms}^{\text{iPr-}}$  and methanol. The ligands fail to coordinate to aqueous molybdate under neutral to acidic conditions. Reaction of  $\text{KTP}^{\text{CO}_2\text{Et,Me}}$  with  $\text{MoO}_2\text{Cl}_2(\text{OPPh}_3)_2$  results in reduction and formation of  $\text{Mo}^{\text{V}}\text{OCl}_3(\text{OPPh}_3)_2 \cdot \text{Mo}^{\text{VI}}\text{O}_2\text{Cl}_2(\text{OPPh}_3)_2$ . The crystal structure of this binary mixture revealed distorted octahedral molecules in crystallographically distinct sites.

**Keywords:** Scorpionate ligands; Molybdenum complexes; Co-crystallization; X-ray crystal structure

## 1. Introduction

Molybdenum enzymes are essential to the health of microorganisms, plants, animals and humans, and are vital agents in many of Earth's biogeochemical cycles [1–4]. Related tungsten enzymes are important to hyperthermophilic organisms found in deep-sea hydrothermal vents and volcanic environments [4, 5]. Molybdenum and tungsten enzymes typically catalyze net oxygen atom transfer (OAT) to or from organic or oxyanionic substrates with concomitant interconversion of Mo(VI) and Mo(IV) enzyme states. Regeneration of the enzyme active sites typically involves sequential one-electron processes featuring coupled electron-proton transfer (CEPT) and the binding or elimination of water, the original source or sink of the transferred oxygen [1–5]. While OAT between biologically relevant Mo(VI) and Mo(IV) states has been extensively studied [6–9], there are few reports of the generation, isolation and study of oxo(aqua)-Mo(IV) and oxo(hydroxo)-Mo(V) complexes [10–13].

Scorpionate complexes feature prominently in spectroscopic and functional models for molybdenum enzymes [8]. Sterically demanding ligands such as hydrotris(3,5-dimethylpyrazol-1-yl)borate ( $\text{Tp}^*$ ; note, the charge is normally omitted on this and related

\*Corresponding author. Email: cgyoung@unimelb.edu.au

ligands) and hydrotris(3-isopropylpyrazol-1-yl)borate ( $\text{Tp}^{\text{iPr}}$ ) limit comproportionation and dinucleation in catalytic, bidirectional OAT reactions and stabilize biologically-relevant, mononuclear Mo(V) species. Some systems feature catalytic substrate oxidation using water as the source of oxygen and the interconversion of Mo(VI), Mo(V) and Mo(IV) complexes via OAT and CEPT reactions. Oxo(aqua)-Mo(IV) and oxo(hydroxo)-Mo(V) complexes are implicated or observed in these systems. However, the isolation (in pure form) and full characterization of these important species has not been realized.

A number of approaches may be envisioned for the synthesis and stabilization of oxo(aqua)- and oxo(hydroxo)-Mo(IV/V) scorpionate complexes. Moving from the current organic solvent systems [8] to aqueous systems would increase the effective concentration of water and assist aqua complex formation and stabilization, e.g. by control of pH. However, this approach requires the synthesis of Mo complexes of water-soluble scorpionate ligands. Progress in this area includes the synthesis of alcohol derivatives of  $\text{HC}(\text{pz})_3$  ( $\text{pz}$ =pyrazol-1-yl) by Reger *et al.* [14] and of tris(pyrazolyl)methanesulfonate ligands,  $\text{Tpms}^-$ , by Kläui *et al.* [15].

Other approaches include hydrogen-bond stabilization of the aqua/hydroxo ligands by hydrogen-bond acceptor/donor groups incorporated into the co-ligands and/or scorpionate. The first of these approaches has failed to deliver stable oxo(aqua)-Mo(IV) complexes [16, 17], although a co-ligand H-bond stabilizing effect has been observed for oxo(hydroxo)- and *cis*-dioxo-Mo(V) complexes [13]. The second approach has met with more success, albeit with first row transition metals rather than Mo. For example the aqua ligand of square-planar  $[\text{Cu}(\text{Tp}^{p\text{-MePy}})(\text{H}_2\text{O})]\text{PF}_6 \cdot \text{CH}_2\text{Cl}_2 \cdot \text{C}_5\text{H}_{12}$  ( $\text{Tp}^{p\text{-MePy}}$  = hydrotris{3-(6-methylpyrid-2-yl)pyrazol-1-yl}borate) is stabilized by intramolecular H-bonding to two pyridyl groups [18], while the Ni, Co, Mn and Cu complexes of the hydrotris(3-carboxyethyl-5-methylpyrazolyl)borate ligand ( $\text{Tp}^{\text{CO}_2\text{Et,Me}}$ ) feature two or three aqua co-ligands stabilized by H-bonding to the ester groups, perchlorate counter ions and/or solvate waters (figure 1) [19]. The latter ligand appears to be well suited to the intramolecular stabilization of aqua co-ligands. It is also noteworthy that the Ni(II) complex,  $[\text{Tp}^{\text{CO}_2\text{Et,Me}}\text{Ni}(\text{H}_2\text{O})_3]\text{ClO}_4$ , is

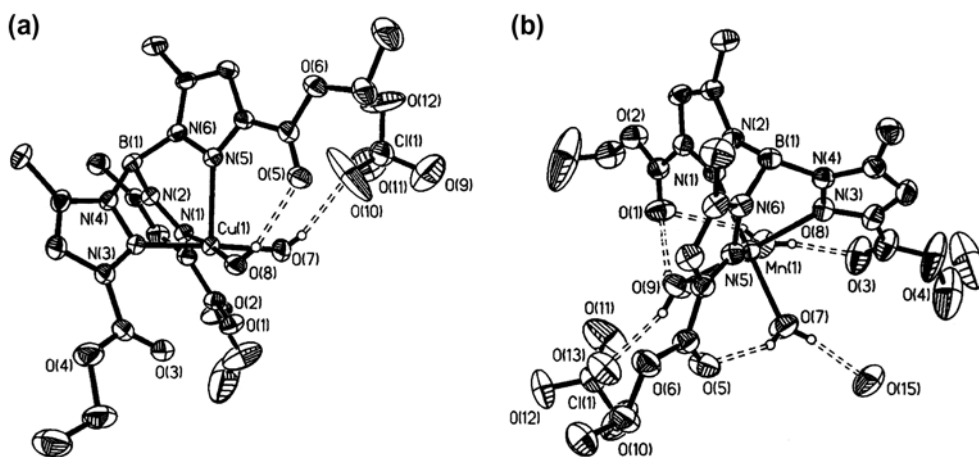


Figure 1. ORTEP projections of the cations of (a)  $[\text{Tp}^{\text{CO}_2\text{Et,Me}}\text{Cu}(\text{H}_2\text{O})_2]\text{ClO}_4$  and (b)  $[\text{Tp}^{\text{CO}_2\text{Et,Me}}\text{Mn}(\text{H}_2\text{O})_3]\text{ClO}_4 \cdot \text{H}_2\text{O}$  (O(15) is a solvent water molecule). Both structures are drawn at the 30% probability level. Adapted from Hammes *et al.* [19] with permission.

highly soluble in polar organic solvents and much less soluble in water due to tight ion-pairing mediated by strong H-bonding between the cation and perchlorate counterion [19].

Here, we report the synthesis of water-soluble lithium and potassium salts of tris(3-isopropylpyrazolyl)methanesulfonate ( $\text{Tpms}^{\text{iPr-}}$ ), the X-ray crystal structure of  $\text{LiTpms}^{\text{iPr-}} \cdot 1.2\text{MeOH}$  and an initial survey of the ligand's coordination chemistry with Mo. Since our initial work in this area [20], Papish *et al.* [21] have reported the synthesis of  $\text{LiTpms}^{\text{iPr-}}$  by a similar method. These workers also prepared  $\text{NaTpms}^{\text{iPr-}}$  and a number of first row transition metal complexes, most of which were characterized by X-ray crystallography [21, 22]; the crystal structure of  $\text{LiTpms}^{\text{iPr-}}$  has not been reported. We also report attempts to prepare Mo complexes from  $\text{KTp}^{\text{CO}_2\text{Et,Me}}$  and the X-ray crystal structure of a by-product of these reactions, viz.,  $\text{Mo}^{\text{V}}\text{OCl}_3(\text{OPPh}_3)_2 \cdot \text{Mo}^{\text{VI}}\text{O}_2\text{Cl}_2(\text{OPPh}_3)_2$ . Our initial survey of the "Mo chemistry" of both ligands suggests that their binding to Mo (in the form of proven starting materials) may be inhibited by competitive ligand protonation (*versus* metallation) or steric factors such as cavity size or functional group encumbrance.

## 2. Experimental

### 2.1. Materials and methods

Analytical reagent grade chemicals and solvents were purchased from commercial suppliers and used without purification. Samples of 3-isopropylpyrazole (3-PrpzH) [10],  $\text{HC}(3\text{-Prpz})_3$  [14], 3-carboxyethyl-5-methylpyrazole [19],  $\text{KTp}^{\text{CO}_2\text{Et,Me}}$  [19],  $\text{MoO}_2\text{Cl}_2(\text{OPPh}_3)_2$  [23] and  $\text{MoO}_2\text{Cl}_2(\text{OH}_2)_2 \cdot \text{H}_2\text{O} \cdot \text{Et}_4\text{NCl}$  [24] were prepared according to literature procedures. The synthesis of 3-carboxyethyl-5-methylpyrazole was modified at the work-up stage, with the reported extraction of product into dichloromethane (which causes product loss) being replaced by pH adjustment to 9–10, followed by filtration and washing of the crystalline product.

Solid-state (KBr disk) infrared spectra were recorded on a Biorad FTS 165 FTIR spectrophotometer.  $^1\text{H}$  NMR spectra were obtained using a Varian Unity Plus 400 spectrometer using external 4,4-dimethyl-4-silapentane-1-sulfonic acid (DSS) ( $\delta 0$ ) or the residual solvent peak ( $\text{DOH } \delta 4.80$ ) as reference. Microanalyses were performed by Atlantic Microlabs Inc., Norcross, GA.

### 2.2. Syntheses

**2.2.1.  $\text{LiTpms}^{\text{iPr-}}$  and  $\text{KTpms}^{\text{iPr-}}$ .** Solid  $\text{HC}(3\text{-Pr'pz})_3$  (10.05 g, 29.5 mmol) was dissolved in dry tetrahydrofuran (100 mL) in a three-necked round-bottom flask. The deep red solution was cooled in an ethanol-dry ice bath and allowed to equilibrate (20 min). *n*-Butyllithium (14.2 mL of a 2.5 M solution in hexanes; 35.5 mmol,  $1.2 \times$  excess) was added by syringe and the mixture stirred at  $-72^\circ\text{C}$  for 1.5 h before sulfur trioxide-trimethylamine,  $\text{SO}_3 \cdot \text{NMe}_3$  (4.945 g, 35.5 mmol,  $1.2 \times$  excess), was added. The final reaction mixture was stirred at  $-72^\circ\text{C}$  for 1.5 h before the ethanol- $\text{CO}_2$  bath was replaced with an ice-water bath. The reaction was stirred for a further 3 h at  $0^\circ\text{C}$  before being transferred to a round-bottomed flask for removal of the solvent and volatiles at  $<30^\circ\text{C}$  on a rotary evaporator. The orange-red fluffy residue was taken up in  $\text{CHCl}_3$  (20 mL, non-distilled) producing a

red solution, from which the product began precipitating within minutes. The mixture was stirred rapidly for 1.5 h and the crude product collected under vacuum and washed with  $\text{CHCl}_3$  (15 mL). Further drying of the crude product under high vacuum yielded 7.69 g of a pale peach solid. Recrystallization from hot methanol afforded colorless crystals of  $\text{LiTpms}^{\text{iPr}}$ . Metathesis of a solution of  $\text{LiTpms}^{\text{iPr}}$  in water–methanol with  $\text{K}_2\text{CO}_3$  afforded the potassium salt,  $\text{KTpms}^{\text{iPr}}$ , in crystalline form upon recrystallization from hot methanol.

$\text{LiTpms}^{\text{iPr}}$ : Anal. Calcd for  $\text{LiTpms}^{\text{iPr}} \cdot 1.2\text{MeOH}$  (%): C, 52.19; H, 6.89; N, 18.08. Found: C, 51.77; H, 6.65; N, 18.39.  $^1\text{H}$  NMR ( $\text{D}_2\text{O}$ ; referenced to external DSS):  $\delta_{\text{H}}$  7.38 (d, 3H,  $J=2.8$ , 5-H of pz); 6.38 (d, 3H,  $J=2.4$ , 4-H of pz); 2.95 (septet, 3H,  $J=6.8$ ,  $\text{CH}(\text{CH}_3)_2$ ); 1.21 (d, 18H,  $J=7.2$ ,  $\text{CH}(\text{CH}_3)_2$ ). FT-IR (KBr,  $\text{cm}^{-1}$ ): 2965 m, 2930 w, 2873 w, 1636 w-m, br, 1535 m, 1473 w-m, 1388 m, 1376 m, 1282 m, 1257 s, 1234 m, 1214 m, 1113 m, 1083 m, 1052 m, 861 m, 766 m, 763 m, 649 m, 470 w-m.

$\text{KTpms}^{\text{iPr}}$ :  $^1\text{H}$  NMR ( $\text{D}_2\text{O}$ ; referenced to HOD):  $\delta_{\text{H}}$  7.39 (d, 3H,  $J=2.4$ , 5-H of pz); 6.40 (d, 3H,  $J=2.8$ , 4-H of pz); 2.96 (septet, 3H,  $J=6.8$ ,  $\text{CH}(\text{CH}_3)_2$ ); 1.23 (d, 18H,  $J=7.2$ ,  $\text{CH}(\text{CH}_3)_2$ ).  $^{13}\text{C}$  NMR ( $\text{D}_2\text{O}$ ; referenced to external DSS):  $\delta_{\text{C}}$  165.5, 135.6, 106.7, 30.0, 24.7. Spectrum with long d1 (first delay) of 40 s:  $\delta_{\text{C}}$  165.7, 164.1 ( $\text{CSO}_3^-$ ), 135.7, 106.8, 30.2, 24.9. FT-IR (KBr,  $\text{cm}^{-1}$ ): 2965 m, 2930 w-m, 2872 w-m, 1633 m, 1534 m, 1401 m, 1371 m, 1251 s, 1214 m, 1068 m, 1050 m, 1008 w-m, 861 m, 757 m, 640 m, 540 m. ESI-MS (cone potential = 10 or 50 V; negative ion mode): 419.42  $[\text{M} - \text{K}^+]^-$  (419.31).

**2.2.2.  $\text{MoOCl}_3(\text{OPPh}_3)_2 \cdot \text{MoO}_2\text{Cl}_2(\text{OPPh}_3)_2$ .** A mixture of  $\text{MoO}_2\text{Cl}_2(\text{OPPh}_3)_2$  (1.0 g, 1.32 mmol) and  $\text{KTp}^{\text{CO}_2\text{Et,Me}}$  (0.64 g, 1.32 mmol) was treated with dry, deoxygenated dichloromethane (20 mL) and stirred for 1 day under anaerobic conditions. The volume of the resultant orange solution was then reduced to 5 mL and diethyl ether (30 mL) was added to precipitate an orange solid, which was collected by filtration (in air) and washed with diethyl ether. The material was recrystallized from dichloromethane–methanol as golden-brown crystals. Addition of ligand was required for formation of  $\text{MoOCl}_3(\text{OPPh}_3)_2 \cdot \text{MoO}_2\text{Cl}_2(\text{OPPh}_3)_2$ . Yield: 0.77 g (95% based on Cl). Anal. Calcd for  $\text{MoOCl}_3(\text{OPPh}_3)_2 \cdot \text{MoO}_2\text{Cl}_2(\text{OPPh}_3)_2$  (%): C, 56.51; H, 3.95; Cl, 11.58. Found: C, 56.31; H, 3.76; Cl, 11.43. FT-IR (KBr,  $\text{cm}^{-1}$ ): 1438 m, 1384 vs, 1370 vs, 1181 m, 1120 m, 1090 w, 1039 w,  $\nu(\text{Mo}=\text{O})$  974 m,  $\nu_{\text{s}}(\text{MoO}_2)$  947 m,  $\nu_{\text{as}}(\text{MoO}_2)$  906 m, 790 m, 738 s, 693 m, 540 s, 483 s. EPR ( $\text{CH}_2\text{Cl}_2$ , 298 K):  $\langle g \rangle = 1.935$ .

### 2.3. X-ray crystallography

Colorless crystals of  $\text{LiTpms}^{\text{iPr}} \cdot 1.2\text{MeOH}$  were obtained by evaporation of a methanol solution of  $\text{LiTpms}^{\text{iPr}}$ . Golden-brown crystals of  $\text{MoOCl}_3(\text{OPPh}_3)_2 \cdot \text{MoO}_2\text{Cl}_2(\text{OPPh}_3)_2$  were obtained by slow diffusion of diethyl ether into a dichloromethane solution of the product obtained from the reaction of  $\text{MoO}_2\text{Cl}_2(\text{OPPh}_3)_2$  with  $\text{KTp}^{\text{CO}_2\text{Et,Me}}$ . For  $\text{LiTpms}^{\text{iPr}} \cdot 1.2\text{MeOH}$ , data were collected at 130(1) K using an Oxford Diffraction Supernova diffractometer with Cu K $\alpha$  radiation. For  $\text{MoOCl}_3(\text{OPPh}_3)_2 \cdot \text{MoO}_2\text{Cl}_2(\text{OPPh}_3)_2$ , data were collected at 293(2) K using a Bruker CCD diffractometer with a sealed tube Mo K $\alpha$  radiation source. The structures were solved using direct methods and refined using the SHELX-97 package of software [25, 26]. Crystal and metrical data are reported in tables 1–3.

Table 1. Crystallographic data.

|  |   |  |
|--|---|--|
| Parameter  | LiTpms <sup>iPr</sup> ·1.2MeOH  | MoOCl <sub>3</sub> (OPPh <sub>3</sub> ) <sub>2</sub> ·MoO <sub>2</sub> Cl <sub>2</sub> (OPPh <sub>3</sub> ) <sub>2</sub> |
| Formula  | C <sub>20.2</sub> H <sub>31.8</sub> LiN <sub>6</sub> O <sub>4.2</sub> S | C <sub>72</sub> H <sub>60</sub> Cl <sub>5</sub> Mo <sub>2</sub> O <sub>7</sub> P <sub>4</sub>                            |
| Formula mass   | 464.92  | 1530.21  |
| Crystal system   | Monoclinic  | Monoclinic   |
| Space group  | C2/c  | P2 <sub>1</sub> /c   |
| a, Å   | 22.7715(7)  | 18.954(2)  |
| b, Å   | 13.4085(3)  | 16.8140(8)   |
| c, Å   | 17.4694(5)  | 22.078(2)  |
| β, °   | 108.909(3)  | 95.851(2)  |
| V, Å <sup>3</sup>  | 5046.1(2)   | 6999.5(13)   |
| Z  | 8   | 4  |
| ρ, g cm <sup>-3</sup>                                    | 1.224   | 1.452  |
| μ, cm <sup>-1</sup>                                      | 1.447   | 6.93   |
| Data (unique data)                                       | 9800 (4995)   | 43,934 (15,898)  |
| R <sub>1</sub> [I > 2σ(I)] <sup>a</sup>                  | 0.0558  | 0.0759   |
| wR <sub>2</sub> (F <sup>2</sup> , all data) <sup>b</sup> | 0.1599  | 0.1644   |
| GOF  | 1.089   | 0.998  |

<sup>a</sup>R<sub>1</sub> = ∑ ||F<sub>o</sub>| - |F<sub>c</sub>|| / ∑ |F<sub>o</sub>|. <sup>b</sup>wR<sub>2</sub> = { [∑ w(F<sub>o</sub><sup>2</sup> - F<sub>c</sub><sup>2</sup>)<sup>2</sup> / ∑ (w|F<sub>o</sub><sup>2</sup>)<sup>2</sup> ] }<sup>1/2</sup>.

Table 2. Selected bond lengths (Å) and angles (°) for LiTpms<sup>iPr</sup>·1.2MeOH<sup>a</sup>.

|                               |           |                               |           |
|-------------------------------|-----------|-------------------------------|-----------|
| Li(1)–N(2)                    | 2.086(3)  | Li(1)–O(2)                    | 1.929(3)  |
| Li(2)–N(6)                    | 2.092(9)  | Li(2)–O(1)                    | 1.904(8)  |
| Li(2)–O(4)                    | 1.843(10) | Li(2)–O(4) <sup>II</sup>      | 1.725(10) |
| O(2)–Li(1)–N(2)               | 95.47(8)  | O(2)–Li(1)–N(2) <sup>I</sup>  | 107.92(8) |
| O(2)–Li(1)–O(2) <sup>I</sup>  | 124.9(3)  | N(2)–Li(1)–N(2) <sup>I</sup>  | 128.3(3)  |
| O(1)–Li(2)–N(6)               | 96.0(4)   | O(1)–Li(2)–O(4)               | 103.9(4)  |
| O(1)–Li(2)–O(4) <sup>II</sup> | 119.0(5)  | N(6)–Li(2)–O(4)               | 118.9(5)  |
| N(6)–Li(2)–O(4) <sup>II</sup> | 109.9(5)  | O(4)–Li(2)–O(4) <sup>II</sup> | 109.1(4)  |

Symmetry operations: <sup>I</sup>1 - x, y, ½ - z; <sup>II</sup>1 - x, 1 - y, -z.

3. Results and discussion

3.1. Synthesis of LiTpms<sup>iPr</sup> and KTpms<sup>iPr</sup>

The method employed by Kläui *et al.* [15] for the synthesis of LiTpms was adapted for the preparation of LiTpms<sup>iPr</sup>. The immediate ligand precursor, tris(3-isopropylpyrazolyl) methane, was produced using the method reported by Reger *et al.* [14]. This compound was converted into LiTpms<sup>iPr</sup> using a one-pot synthesis involving sequential lithiation (using *n*-butyllithium) and sulfonation (using SO<sub>3</sub>·NMe<sub>3</sub>) reactions [15]. The potassium salt was prepared by the metathetical reaction of LiTpms<sup>iPr</sup> with potassium carbonate.

3.2. Crystal structure of LiTpms<sup>iPr</sup>·1.2MeOH

The asymmetric unit of LiTpms<sup>iPr</sup>·1.2MeOH consists of a single anion, two crystallographically distinct Li centers and two types of methanol, one a full occupancy ligand and the other a sub-occupancy solvate [figure 2(a)]. The lithium centers exhibit two distinct coordination environments. As indicated in figure 2(b), Li(1) is coordinated by a pair of symmetry related, chelate κ<sup>2</sup>N,O-Tpms<sup>iPr-</sup> anions. Atom Li(1), which is located on a 2-fold axis, is in a



Table 3. Selected bond lengths (Å) and angles (°) for  $\text{MoOCl}_3(\text{OPPh}_3)_2 \cdot \text{MoO}_2\text{Cl}_2(\text{OPPh}_3)_2$ .

|                   |            |                   |            |
|-------------------|------------|-------------------|------------|
| Mo(1)–O(1)        | 1.667(4)   | Mo(2)–O(4)        | 1.752(4)   |
| Mo(1)–O(2)        | 2.158(3)   | Mo(2)–O(5)        | 1.722(4)   |
| Mo(1)–O(3)        | 2.099(3)   | Mo(2)–O(6)        | 2.190(3)   |
| Mo(1)–Cl(1)       | 2.271(2)   | Mo(2)–O(7)        | 2.180(4)   |
| Mo(1)–Cl(2)       | 2.3902(16) | Mo(2)–Cl(4)       | 2.3877(17) |
| Mo(1)–Cl(3)       | 2.3884(16) | Mo(2)–Cl(5)       | 2.3942(17) |
| O(1)–Mo(1)–O(2)   | 174.31(16) | O(4)–Mo(2)–O(5)   | 100.74(19) |
| O(1)–Mo(1)–O(3)   | 94.61(16)  | O(4)–Mo(2)–O(6)   | 89.95(17)  |
| O(1)–Mo(1)–Cl(1)  | 99.65(15)  | O(4)–Mo(2)–O(7)   | 168.85(17) |
| O(1)–Mo(1)–Cl(2)  | 93.88(15)  | O(4)–Mo(2)–Cl(4)  | 93.85(15)  |
| O(1)–Mo(1)–Cl(3)  | 96.36(15)  | O(4)–Mo(2)–Cl(5)  | 83.75(10)  |
| O(2)–Mo(1)–O(3)   | 79.70(13)  | O(5)–Mo(2)–O(6)   | 169.30(17) |
| O(2)–Mo(1)–Cl(1)  | 86.03(10)  | O(5)–Mo(2)–O(7)   | 90.41(17)  |
| O(2)–Mo(1)–Cl(2)  | 85.59(10)  | O(5)–Mo(2)–Cl(4)  | 94.85(14)  |
| O(2)–Mo(1)–Cl(3)  | 84.64(11)  | O(5)–Mo(2)–Cl(5)  | 94.61(14)  |
| O(3)–Mo(1)–Cl(1)  | 165.69(11) | O(6)–Mo(2)–O(7)   | 78.90(14)  |
| O(3)–Mo(1)–Cl(2)  | 86.08(11)  | O(6)–Mo(2)–Cl(4)  | 84.91(10)  |
| O(3)–Mo(1)–Cl(3)  | 87.40(11)  | O(6)–Mo(2)–Cl(5)  | 83.75(10)  |
| Cl(1)–Mo(1)–Cl(2) | 91.78(7)   | O(7)–Mo(2)–Cl(4)  | 85.34(11)  |
| Cl(1)–Mo(1)–Cl(3) | 92.38(7)   | O(7)–Mo(2)–Cl(5)  | 83.53(11)  |
| Cl(2)–Mo(1)–Cl(3) | 169.09(6)  | Cl(4)–Mo(2)–Cl(5) | 165.43(6)  |
| Mo(1)–O(2)–P(1)   | 168.6(2)   | Mo(2)–O(6)–P(3)   | 165.4(2)   |
| Mo(1)–O(3)–P(2)   | 146.0(2)   | Mo(2)–O(7)–P(4)   | 162.5(2)   |

distorted tetrahedral  $\text{N}_2\text{O}_2$  environment with angles of  $95.47(8)$ – $128.3(3)^\circ$  subtended at Li(1). In contrast, Li(2) is coordinated by only one  $\kappa^2\text{N},\text{O}$ -Tpms<sup>IPr</sup> anion and a pair of symmetry related methanol molecules (O(4)–C(20)) located on either side of an inversion center. Two sites for Li(2) are located close to the inversion center but only one of the sites is occupied at any one time; the two Li(2) sites are only  $2.07(2)$  Å apart. The symmetry related Li(2) sites, one of which is indicated by cross-hatching, are indicated in figure 2(c). The methanol oxygen (O(4)) is located only  $2.952(3)$  Å from the sulfonate oxygen (O(1)), a separation that is consistent with the presence of a weak hydrogen bond when the Li(2) site is empty.

The isopropylpyrazolyl group containing N(2) is disordered and adopts two orientations, with C(2), N(1) and N(2) occupying the same sites in both orientations. The major orientation is shown in figure 2(a). The minor orientation is located near the 2-fold axis through Li(1) and as a result there is insufficient space for the anion and its symmetry related neighbor to both be in the minor orientation at the same time. When both of the symmetry related molecules have the isopropylpyrazolyl group in the major orientation, a sub-occupancy, disordered methanol molecule occupies a site near the 2-fold axis. The site occupancy of this methanol refines to a value just under 20%. The isopropyl substituent of C(10) is also disordered, with methyls occupying two sets of sites.

The Li–N contacts of  $2.086(3)$  and  $2.092(9)$  Å are similar to those reported for trigonally coordinated Li in  $[\text{PhTp}^{\text{t-Bu}}]\text{Li}$  ( $1.934$ – $1.979$  Å) [27], and the Li–N bonds of octahedrally coordinated Li in  $[\text{HC}(3,5\text{-Me}_2\text{pz})_3]\text{Li}(\eta^3\text{-BH}_4)$  (two bonds at  $2.038$  Å and the third at  $2.092$  Å) [28]. The Li–O<sub>sulfonate</sub> distances of  $1.904(8)$  and  $1.929(3)$  Å are typical of Li–O bonds; the Li–O<sub>methanol</sub> bonds ( $1.725(10)$  and  $1.843(10)$  Å) are shorter than reported Li–O bond distances for non-bridging methanol donors ( $1.900$ – $1.906$  Å) [29, 30]. The S–O bonds of the sulfonate are all very similar and lie in the range of  $1.437(2)$  to  $1.449(2)$  Å. The sulfur has a slightly distorted tetrahedral geometry, with O–S–O angles of  $113.17(10)$  to  $115.48(11)^\circ$  and O–S–C angles  $103.42(9)$  to  $104.48(10)^\circ$ .



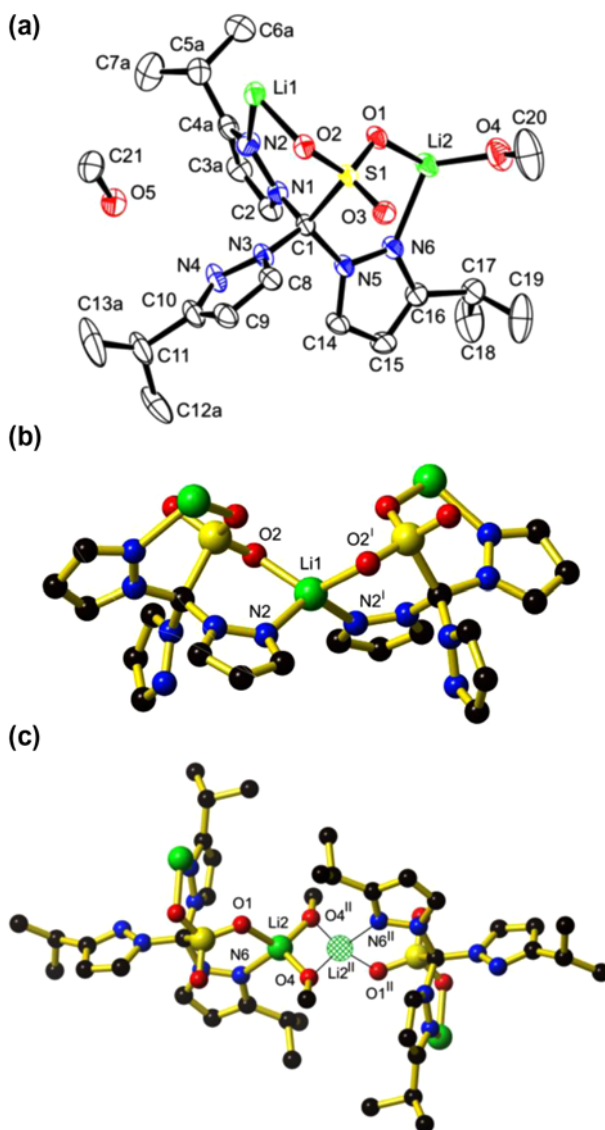


Figure 2. The structure of  $\text{LiTpms}^{i\text{Pr}} \cdot 1.2\text{MeOH}$ . (a) An ORTEP diagram showing the asymmetric unit with probability ellipsoids represented at the 30% level. (b) A ball and stick representation highlighting the coordination environment of Li(1); isopropyl groups have been omitted for clarity. (c) A ball and stick representation highlighting the coordination environment of Li(2); two locations for Li(2) are indicated (one with cross-hatching) but only one of the two indicated Li(2) centers is present at any one time. In all three figures, only the major conformation of the anion is indicated. All hydrogens have been omitted for clarity. Symmetry operations: I  $1-x, y, \frac{1}{2}-z$ ; II  $1-x, 1-y, -z$ . Color code: S yellow; O red; N blue; C black; Li green. (see <http://dx.doi.org/10.1080/00206814.2013.778988> for color version).

The structure of  $\text{LiTpms}^{i\text{Pr}} \cdot 1.2\text{MeOH}$  contrasts with that reported [21] for  $\text{NaTpms}^{i\text{Pr}}$ , which exhibits a tetrameric structural unit, with two unique sodium centers related by an inversion center. Each of the sodium centers is six-coordinate, with a distorted octahedral geometry; coordination of the ligand is via bridging and non-bridging pyrazole nitrogen

and sulfonate oxygens. We believe salts of  $\text{Tpms}^{\text{iPr}-}$  can adopt a variety of solid-state structures depending on the cation, solvents present and crystallization conditions.

### 3.3. Reactions of $(\text{Li/K})\text{Tpms}^{\text{iPr}}$ with oxo-molybdenum species

Acidification of a mixture of  $\text{LiTpms}^{\text{iPr}}$  and  $\text{Na}_2\text{MoO}_4$  (0.06 M each) in  $\text{D}_2\text{O}$  using 1.25 M  $\text{DCl}$  in  $\text{D}_2\text{O}$  was monitored by  $^1\text{H}$  NMR spectroscopy. No changes in the chemical shifts of the ligand were observed up to the point where ligand precipitation occurred. This indicates that water soluble  $\text{LiTpms}^{\text{iPr}}$  did not react with  $\text{Na}_2\text{MoO}_4$  under conditions expected to generate reactive  $[\text{MoO}_2]^{2+}(\text{aq})$  species. Reaction of equimolar amounts of  $\text{KTpms}^{\text{iPr}}$  and  $\text{MoO}_2\cdot\text{Cl}_2(\text{OH}_2)_2\cdot\text{H}_2\text{O}\cdot\text{Et}_4\text{NCl}$  in water–methanol mixtures produced a slightly off-white solid. The  $^1\text{H}$  NMR spectrum of the solid (in  $\text{D}_2\text{O}$  or  $\text{d}_6$ -acetone) revealed the presence of uncomplexed ligand, along with the tetraethylammonium cation. The infrared spectrum revealed four bands in the  $\nu(\text{Mo}=\text{O})$  region, two of which correlated with the presence of the Mo-containing starting material. The remaining two bands ( $933$  and  $900\text{ cm}^{-1}$ ) indicate the co-precipitation of molybdate, as  $(\text{Et}_4\text{N})_2[\text{MoO}_4]$ . Hence, the material obtained was identified as a mixture of  $\text{KTpms}^{\text{iPr}}$ ,  $\text{MoO}_2\text{Cl}_2(\text{OH}_2)_2$  and  $(\text{Et}_4\text{N})_2[\text{MoO}_4]$ .

### 3.4. Reactions of $\text{KTp}^{\text{CO}_2\text{Et,Me}}$ with molybdenum species

Reaction of potassium trispyrazolylborate salts ( $\text{KTp}^x$ ) with  $\text{Mo}(\text{CO})_6$ , followed by addition of  $\text{NEt}_4\text{Cl}$ , leads to the formation of  $\text{NEt}_4[\text{Tp}^x\text{Mo}(\text{CO})_3]$ . The reaction can be conveniently monitored by solution IR spectroscopy, with two strong  $\nu(\text{CO})$  bands in the  $2250\text{--}1950\text{ cm}^{-1}$  region being indicative of the formation of the  $\text{C}_{3v}$  anion [31]. However, reaction of  $\text{KTp}^{\text{CO}_2\text{Et,Me}}$  with  $\text{Mo}(\text{CO})_6$  in DMF resulted in the loss of the  $\nu(\text{CO})$  bands of  $\text{Mo}(\text{CO})_6$  without any appearance of bands assignable to  $[\text{Tp}^{\text{CO}_2\text{Et,Me}}\text{Mo}(\text{CO})_3]^-$  or any other carbonyl species. Attempted work-up of the reaction yielded an intractable mixture of unidentified products.

Reaction of equimolar quantities of  $\text{MoO}_2\text{Cl}_2(\text{OPPh}_3)_2$  and  $\text{KTp}^{\text{CO}_2\text{Et,Me}}$  in dichloromethane under anaerobic conditions produced an orange/brown solution yielding a brown crystalline solid upon work-up (“molybdenum blues” are observed to form in the absence of ligand). IR spectroscopy revealed an absence of bands assignable to the  $\text{Tp}^{\text{CO}_2\text{Et,Me}}$  ligand but the presence of bands indicative of  $\text{OPPh}_3$  ligation to Mo. The IR spectrum also exhibited bands attributable to  $\nu_s(\text{MoO}_2)$  and  $\nu_{as}(\text{MoO}_2)$  stretches of  $\text{MoO}_2\text{Cl}_2(\text{OPPh}_3)_2$  ( $947$  and  $906\text{ cm}^{-1}$ , respectively) [23] and the  $\nu(\text{MoO})$  stretching mode of  $\text{MoOCl}_3(\text{OPPh}_3)_2$  ( $974\text{ cm}^{-1}$ ) [32]. The  $^1\text{H}$  NMR spectrum of the compound revealed broadened signals assignable to triphenylphosphine oxide. EPR spectroscopy indicated the presence of an Mo(V)  $\text{d}^1$  complex, the  $g$  value observed (1.935) being the same as that reported by Garner *et al.* for  $\text{MoOCl}_3(\text{OPPh}_3)_2$  [33]. The compound was, therefore, formulated as a mixture of  $\text{Mo}^{\text{V}}\text{OCl}_3(\text{OPPh}_3)_2$  and  $\text{Mo}^{\text{VI}}\text{O}_2\text{Cl}_2(\text{OPPh}_3)_2$ .

### 3.5. Crystal structure of $\text{MoOCl}_3(\text{OPPh}_3)_2\cdot\text{MoO}_2\text{Cl}_2(\text{OPPh}_3)_2$

X-ray crystallography established the compound to be a 1:1 binary mixture of  $\text{Mo}^{\text{V}}\text{OCl}_3(\text{OPPh}_3)_2$  and  $\text{Mo}^{\text{VI}}\text{O}_2\text{Cl}_2(\text{OPPh}_3)_2$ . A view of the asymmetric unit is shown in figure 3 and selected bond distances and angles are contained in table 3.

Two polymorphs of pure  $\text{MoOCl}_3(\text{OPPh}_3)_2$  have been structurally characterized. The first, crystallized in space group  $P2_1/c$ , contained two distorted octahedral molecules in the asymmetric unit [33]. One of these molecules was ordered and will be employed in the structural comparisons to follow. The other exhibited two-site, positional disorder with oxo and chloro ligands distributed equally over the two sites.

The second polymorph, in space group  $C2/c$ , also displayed positional disorder within the crystallographically unique distorted octahedral molecule; in this case oxo and chloride positions were resolved but the associated Mo–L distances were not reliable [34]. The Mo (V) component of the title structure has bond lengths and angles (table 3) that are essentially the same as those of the ordered molecule in the structures above. The Mo(1)–O(1) distance of 1.667(4) Å is typical of molybdenyl compounds and compares well with the published value of 1.662(13) Å for pure  $\text{MoOCl}_3(\text{OPPh}_3)_2$  [33]. A notable difference is found in Mo(1)–Cl(1) distances, that of the title compound and ordered  $\text{MoOCl}_3(\text{OPPh}_3)_2$  being 2.271(2) and 2.348(5) Å [33], respectively. Two-site disorder of oxo and *cis*-chloro ligands would introduce a pseudo- $C_2$  axis through the midpoints of the  $\text{OPPh}_3 \cdots \text{OPPh}_3$  and  $\text{O/Cl} \cdots \text{O/Cl}$  donor sites, resulting in equalization of the Mo– $\text{OPPh}_3$  distances and the “Mo–O/Cl” distances (assuming the atoms are not resolved [34, 35]). Clearly, the data presented here (table 3) are not consistent with the effects of a two-site ligand disorder. Residual electron density observed around Mo(1) is less than  $0.8 \text{ e}^-/\text{\AA}^3$  at each site, with the closest

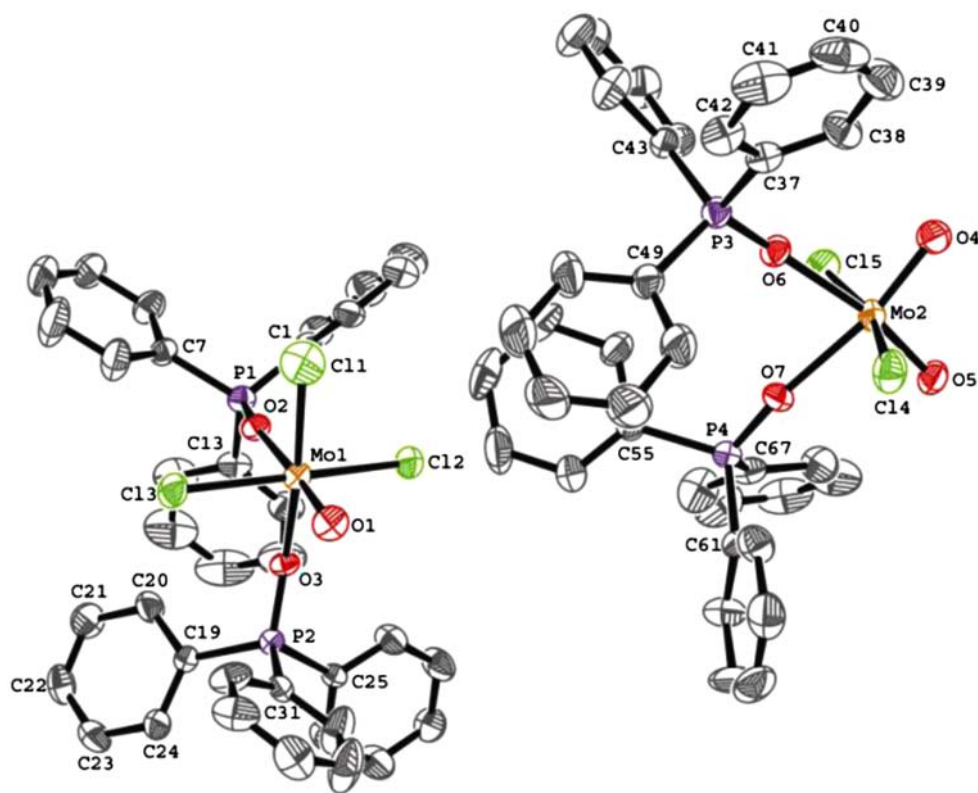


Figure 3. ORTEP projection of co-crystallized  $\text{Mo}^{\text{V}}\text{OCl}_3(\text{OPPh}_3)_2 \cdot \text{Mo}^{\text{VI}}\text{O}_2\text{Cl}_2(\text{OPPh}_3)_2$ . Probability ellipsoids are drawn at the 30% level.

to Cl(1) being 1.22 Å away. As the structure is well ordered, the suspect Mo(1)–Cl(1) distance is likely to result from a small degree of compositional disorder between MoOCl<sub>3</sub>(OPPh<sub>3</sub>)<sub>2</sub> and MoO<sub>2</sub>Cl<sub>2</sub>(OPPh<sub>3</sub>)<sub>2</sub>, of the type demonstrated by Parkin [36, 37] and Fronczek *et al.* [38].

The crystal structure of pure MoO<sub>2</sub>Cl<sub>2</sub>(OPPh<sub>3</sub>)<sub>2</sub> was reported by Butcher *et al.* [23]. The complex displays a distorted octahedral geometry, with average Mo=O, Mo–Cl and Mo–OPPh<sub>3</sub> distances of 1.684, 2.392 and 2.185 Å, respectively. The corresponding parameters for the bromo analog, MoO<sub>2</sub>Br<sub>2</sub>(OPPh<sub>3</sub>)<sub>2</sub>, are 1.69–1.73(1), 2.548 and 2.18 Å, respectively [23]. Short Mo=O bond distances have also been reported for *inter alia* MoO<sub>2</sub>Cl<sub>2</sub>(OPMePh<sub>2</sub>)<sub>2</sub> (av. 1.677(3) Å) [38] MoO<sub>2</sub>X<sub>2</sub>(OPMe<sub>3</sub>)<sub>2</sub> (X = Cl (1.685(3) Å), Br (1.691(3) Å)), MoO<sub>2</sub>Br<sub>2</sub>{*o*-C<sub>6</sub>H<sub>4</sub>(P(O)Ph<sub>2</sub>)<sub>2</sub>} (1.694(3) Å) and MoO<sub>2</sub>Cl<sub>2</sub>{Ph<sub>2</sub>P(O)CH<sub>2</sub>P(O)Ph<sub>2</sub>} (av. 1.696 Å) [39]. The Mo(VI) component of the title compound also exhibits a distorted octahedral geometry, the bond distances and angles (table 3) being similar to those reported for pure MoO<sub>2</sub>Cl<sub>2</sub>(OPPh<sub>3</sub>)<sub>2</sub> [23]. The most notable difference in the two structures is the apparent lengthening of the Mo=O bonds (at 1.722(4) and 1.752(4) Å) in the title complex compared to those of pure MoO<sub>2</sub>Cl<sub>2</sub>(OPPh<sub>3</sub>)<sub>2</sub> and related compounds (the 1.73(1) Å Mo=O distance in pure MoO<sub>2</sub>Br<sub>2</sub>(OPPh<sub>3</sub>)<sub>2</sub> being a notable exception). Again, it is likely that compositional disorder between MoOCl<sub>3</sub>(OPPh<sub>3</sub>)<sub>2</sub> and MoO<sub>2</sub>Cl<sub>2</sub>(OPPh<sub>3</sub>)<sub>2</sub> (the complement to that discussed above for the second crystallographically unique site) accounts for the apparent lengthening in the Mo=O distances. It is difficult to assess the degree of compositional disorder in the absence of the full resolution of the atomic positions but it is estimated to be small (<5%). A full discussion of the crystallographic ramifications of compositional and ligand disorder has been provided by Parkin [36, 37].

The co-crystallization of MoOCl<sub>3</sub>(OPPh<sub>3</sub>)<sub>2</sub> and MoO<sub>2</sub>Cl<sub>2</sub>(OPPh<sub>3</sub>)<sub>2</sub>, with attendant changes in product color (ranging from orange to green), was first noted by Horner and Tyree in 1962 [32]. The closely related complexes, MoOCl<sub>3</sub>(OPMePh<sub>2</sub>)<sub>2</sub> and MoO<sub>2</sub>Cl<sub>2</sub>(OPMePh<sub>2</sub>)<sub>2</sub>, as well as MoOCl<sub>3</sub>(OPMe<sub>2</sub>Ph)<sub>2</sub> and MoCl<sub>4</sub>(OPMe<sub>2</sub>Ph)<sub>2</sub>, also form binary mixtures that have been characterized by X-ray crystallography [38]. Indeed, co-crystallization is a common feature of chloro-Mo complexes containing bulky P-containing co-ligands, particularly phosphine oxides; some other examples include MoCl<sub>3</sub>(OPPh<sub>3</sub>)<sub>2</sub>(NO)·MoCl<sub>4</sub>(OPPh<sub>3</sub>)<sub>2</sub> [40], MoO<sub>2</sub>Cl<sub>2</sub>(OPPh<sub>3</sub>)<sub>2</sub>·MoOSCl<sub>2</sub>(OPPh<sub>3</sub>)<sub>2</sub> [41], mixtures of MoO<sub>2</sub>Cl<sub>2</sub>(OPPh<sub>3</sub>)<sub>2</sub> and MoO(O<sub>2</sub>)Cl<sub>2</sub>(OPPh<sub>3</sub>)<sub>2</sub> [42], and the original examples of “bond-stretch isomerism”, which were shown to be binary mixtures of MoOCl<sub>2</sub>(PMe<sub>2</sub>Ph)<sub>3</sub> and MoCl<sub>3</sub>(PMe<sub>2</sub>Ph)<sub>3</sub> [43, 44].

#### 4. Summary

Three water-soluble scorpionate ligands, viz., (Li/K)Tpms<sup>iPr</sup> and KTp<sup>CO<sub>2</sub>Et,Me</sup>, have been prepared and their reactions with Mo-containing complexes have been investigated. The X-ray crystal structure of LiTpms<sup>iPr</sup>·1.2MeOH is reported. The ligands fail to react with a variety of common Mo containing starting materials. The reason for this lack of reactivity is unclear but could involve preferential protonation, rather than metallation, under the conditions employed or an energetically unfavorable mis-match in the size of the metal and ligand cavity. A product of the reaction of MoO<sub>2</sub>Cl<sub>2</sub>(OPPh<sub>3</sub>)<sub>2</sub> with KTp<sup>CO<sub>2</sub>Et,Me</sup> has been structurally characterized as the binary mixture Mo<sup>V</sup>OCl<sub>3</sub>(OPPh<sub>3</sub>)<sub>2</sub>·Mo<sup>VI</sup>O<sub>2</sub>Cl<sub>2</sub>(OPPh<sub>3</sub>)<sub>2</sub>. Unfortunately, the inability to obtain dioxo-Mo(VI) complexes of either ligand has thwarted attempts to generate water-soluble, H-bond stabilized oxo(aqua)-Mo(IV) and oxo(hydroxo)-Mo(V) complexes of these ligands as Mo enzyme models.

## Supplementary material

CCDC 876393 and 876394, respectively, contain the supplementary crystallographic data for  $\text{LiTpms}^{\text{iPr}} \cdot 1.2\text{MeOH}$  and  $\text{MoOCl}_3(\text{OPPh}_3)_2 \cdot \text{MoO}_2\text{Cl}_2(\text{OPPh}_3)_2$ . These data can be obtained free of charge via <http://www.ccdc.cam.ac.uk/conts/retrieving.html>, or from the Cambridge Crystallographic Data Center, 12 Union Road, Cambridge CB2 1EZ, UK; Fax: (+44) 1223 336 033; or E-mail: [deposit@ccdc.cam.ac.uk](mailto:deposit@ccdc.cam.ac.uk).

## Acknowledgements

We thank Ms Sally Duck (Monash University) for mass spectrometric data and gratefully acknowledge the financial support from the Australian Research Council and the Donors of the Petroleum Research Fund (administered by the American Chemical Society).

## References

- [1] R. Hille. *Chem. Rev.*, **96**, 2757 (1996).
- [2] J.M. Tunney, J. McMaster, C.D. Garner. In *Comprehensive Coordination Chemistry II*, J.A. McCleverty, T.J. Meyer (Eds.), Vol. 8, Chap. 8.18, pp. 459–477, Elsevier-Pergamon, Amsterdam (2004).
- [3] C.G. Young. In *Encyclopedia of Inorganic Chemistry 2*, R.B. King (Ed.), Vol. V, pp. 3321–3340, Wiley, Chichester (2005).
- [4] M.J. Romão. *Dalton Trans.*, 4053 (2009).
- [5] M.K. Johnson, D.C. Rees, M.W.W. Adams. *Chem. Rev.*, **96**, 2817 (1996).
- [6] R.H. Holm. *Chem. Rev.*, **87**, 1401 (1987).
- [7] R.H. Holm. *Coord. Chem. Rev.*, **100**, 183 (1990).
- [8] C.G. Young. In *Biomimetic Oxidations Catalyzed by Transition Metal Complexes*, B. Meunier (Ed.), pp. 415–459, Imperial College Press, London (2000).
- [9] P. Basu, V.N. Nemykin, R.S. Sengar. *Inorg. Chem.*, **48**, 6303 and references cited therein (2009).
- [10] Z. Xiao, M.A. Bruck, C. Doyle, J.H. Enemark, C. Grittini, R.W. Gable, A.G. Wedd, C.G. Young. *Inorg. Chem.*, **34**, 5950 (1995) (Erratum: *ibid.* **35**, 5752 (1996)).
- [11] Z. Xiao, R.W. Gable, A.G. Wedd, C.G. Young. *J. Am. Chem. Soc.*, **118**, 2912 (1996).
- [12] C.G. Young, L.J. Laughlin, S. Colmanet, S.D.B. Scrofanì. *Inorg. Chem.*, **35**, 5368 (1996).
- [13] V.W.L. Ng, M.K. Taylor, J.M. White, C.G. Young. *Inorg. Chem.*, **49**, 9460 (2010).
- [14] D.L. Reger, T.C. Grattan, K.J. Brown, C.A. Little, J.J.S. Lamba, A.L. Rheingold, R.D. Sommer. *J. Organomet. Chem.*, **607**, 120 (2000).
- [15] W. Kläui, M. Berghahn, G. Rheinwald, H. Lang. *Angew. Chem., Int. Ed.*, **39**, 2464 (2000).
- [16] L.M.R. Hill, M.K. Taylor, V.W.L. Ng, C.G. Young. *Inorg. Chem.*, **47**, 1044 (2008).
- [17] V.W.L. Ng, M.K. Taylor, C.G. Young. *Inorg. Chem.*, **51**, 3202 (2012).
- [18] E.R. Humphrey, K.L.V. Mann, Z.R. Reeves, A. Behrendt, J.C. Jeffery, J.P. Maher, J.A. McCleverty, M.D. Ward. *New J. Chem.*, **23**, 417 (1999).
- [19] B.S. Hammes, M.W. Carrano, C.J. Carrano. *J. Chem. Soc., Dalton Trans.*, 1448 (2001).
- [20] L.M.R. Hill. Molybdenum chemistry: bioinorganic meets polyoxometallic. PhD thesis, University of Melbourne (2004).
- [21] E.T. Papish, M.T. Taylor, F.E.I. Jernigan, M.J. Rodig, R.R. Shawhan, G.P.A. Yap, F.A. Jové. *Inorg. Chem.*, **45**, 2242 (2006).
- [22] F.E. Jernigan, F.A. Jové, E.T. Papish, G.P.A. Yap. *Acta Cryst., Sect. E*, **62**, m3172 (2006).
- [23] R.J. Butcher, B.R. Penfold, E. Sinn. *J. Chem. Soc., Dalton Trans.*, 668 (1979).
- [24] M.J. Taylor, W. Jirong, C.E.F. Rickard. *Polyhedron*, **12**, 1433 (1993).
- [25] G.M. Sheldrick. *SHELXS-97 Program for Crystal Structure Solution*, University of Göttingen, Germany (1997).
- [26] G.M. Sheldrick. *SHELXL-97 Program for Crystal Structure Refinement*, University of Göttingen, Germany (1997).
- [27] J.L. Kisko, T. Hascall, C. Kimblin, G. Parkin. *J. Chem. Soc., Dalton Trans.*, 1929 (1999).
- [28] D.L. Reger, J.E. Collins, M.A. Matthews, A.L. Rheingold, L.M. Liable-Sands, I.A. Guzei. *Inorg. Chem.*, **36**, 6266 (1997).
- [29] M.C. Etter, G. Ranawake. *J. Am. Chem. Soc.*, **114**, 4430 (1992).

- [30] Z.A. Starikova, E.P. Turevskaya, N.Y. Turova, A.I. Yanovsky. *J. Chem. Soc., Dalton Trans.*, 3237 (2000).
- [31] S. Trofimenko. *Scorpionates: The Coordination Chemistry of Polypyrazolylborate Ligands*, Imperial College Press, London (1999).
- [32] S.M. Horner, S.Y.J. Tyree. *Inorg. Chem.*, **1**, 122 (1962).
- [33] C.D. Garner, N.C. Howlader, F.E. Mabbs, A.T. McPhail, K.D. Onan. *J. Chem. Soc., Dalton Trans.*, 1848 (1978).
- [34] B.E. Owens, R. Poli. *Acta Crystallogr.*, **C48**, 2137 (1992).
- [35] F.A. Cotton, M. Kohli, R.L. Luck, J.V. Silverton. *Inorg. Chem.*, **32**, 1868 (1993).
- [36] G. Parkin. *Acc. Chem. Res.*, **25**, 455 (1992).
- [37] G. Parkin. *Chem. Rev.*, **93**, 887 (1993).
- [38] F.R. Fronczek, R.L. Luck, G. Wang. *Inorg. Chim. Acta*, **342**, 247 (2003).
- [39] M.B. Hursthouse, W. Levason, R. Ratnani, G. Reid. *Polyhedron*, **23**, 1915 (2004).
- [40] G. Philipp, S. Wocadlo, W. Massa, K. Dehnicke, D. Fenske, C. Maichle-Mössmer, E. Niquet, J. Strähle. *Z. Naturforsch.*, **B50**, 1 (1995).
- [41] G.V. Romanenko, N.V. Podberezskaya, V.P. Fedin, O.A. Geras'ko, V.E. Fedorov, V.V. Bakakin. *Z. Stuk. Khim. (Trans.)*, **29**, 79 (1988).
- [42] G. Wang, A. Jimtaisong, R.L. Luck. *Inorg. Chim. Acta*, **358**, 933 (2005).
- [43] K. Yoon, G. Parkin, A.L. Rheingold. *J. Am. Chem. Soc.*, **113**, 1437 (1991).
- [44] P.J. Desrochers, K.W. Nebesny, M.J. LaBarre, S.E. Lincoln, T.M. Loehr, J.H. Enemark. *J. Am. Chem. Soc.*, **113**, 9193 (1991).